Impact of Aerosols on Atmospheric Attenuation Loss in Central Receiver Systems

Preprint

Manajit Sengupta and Michael J. Wagner

To be presented at SolarPACES 2011
Granada, Spain
September 20-23, 2011

NREL is a national laboratory of the U.S. Department of Energy, Office of Energy Efficiency & Renewable Energy, operated by the Alliance for Sustainable Energy, LLC.

Conference Paper
NREL/CP-5500-52487
August 2011

Contract No. DE-AC36-08GO28308

Available electronically at http://www.osti.gov/bridge

Available for a processing fee to U.S. Department of Energy and its contractors, in paper, from:

U.S. Department of Energy
Office of Scientific and Technical Information

P.O. Box 62
Oak Ridge, TN 37831-0062
phone: 865.576.8401
fax: 865.576.5728
email: mailto:reports@adonis.osti.gov

Available for sale to the public, in paper, from:

U.S. Department of Commerce
National Technical Information Service
5285 Port Royal Road
Springfield, VA 22161
phone: 800.553.6847
fax: 703.605.6900
email: orders@ntis.fedworld.gov
online ordering: http://www.ntis.gov/help/ordermethods.aspx

Cover Photos: (left to right) PIX 16416, PIX 17423, PIX 16560, PIX 17613, PIX 17436, PIX 17721

Printed on paper containing at least 50% wastepaper, including 10% post consumer waste.

IMPACT OF AEROSOLS ON ATMOSPHERIC ATTENUATION LOSS IN CENTRAL RECEIVER SYSTEMS

Manajit Sengupta[1] and Michael J. Wagner[2]

(1) Ph.D., Senior Scientist, National Renewable Energy Laboratory, MS 5202, 1617 Cole Blvd, Golden, CO 80401, USA, +1 303 275 3706, Manajit.Sengupta@nrel.gov
(2) National Renewable Energy Laboratory, MS 5202, 1617 Cole Blvd, Golden, CO 80401, USA

ABSTRACT

Atmospheric attenuation loss between the heliostat field and receiver has been recognized as a significant source of loss in Central Receiver Systems. In clear sky situations, extinction of Direct Normal Irradiance (DNI) is primarily by aerosols in the atmosphere. When aerosol loading is high close to the surface the attenuation loss between heliostat and receivers is significantly influenced by the amount of aerosols present on a particular day. This study relates measured DNI to aerosol optical depths close to the surface of the earth. The model developed in the paper uses only measured DNI to estimate the attenuation between heliostat and receiver in a central receiver system. The requirement that only a DNI measurement is available potentially makes the model a candidate for widespread use.

Keywords: DNI, Attenuation Loss, Heliostat, Central Receiver, Aerosols

1. INTRODUCTION

Atmospheric attenuation loss between the heliostat field and receiver has long been recognized as a significant source of loss in Central Receiver Systems. Attenuation losses can potentially reach over 10% especially as distances between heliostats and receivers reach distances of a kilometer or more. Historically this loss has been represented by parametric equations that are functions of distance between heliostat and receiver [1],[2],[3][4][5] with separate equations for different levels of aerosol loading. Individual equations do not directly account for variability in aerosols, which is the primary source of DNI losses close to the surface where most of the transmission between heliostat and receiver occurs. It is therefore possible that a model that directly accounts for aerosol variability close to the surface will lead to a better estimate of attenuation losses between heliostat and receiver. In this paper we build a model that directly accounts for aerosol variability with the expectation that it will provide a more accurate representation of the attenuation loss.

To get the most accurate estimate of attenuation between heliostat and receiver it is necessary to measure aerosol optical properties as well as water vapor mixing ratio profiles in the first few hundred meters from the surface where the heliostat and receiver lies. Such measurements are expensive and therefore generally not available. The other option is to obtain an estimate of aerosol optical depths close to the surface using available measurements. Making use of the fact that DNI measurements are generally available at central receiver system this study seeks to model attenuation loss close to the surface as a function of measured DNI. The theory and methodology behind this work is summarized in Section 2. Section 3 presents the results of the calculations and the model while Section 4 provides a brief summary and a description of future work.

2. METHODOLOGY

In clear sky situations, extinction of Direct Normal Irradiance (DNI) through either absorption or scattering is primarily from aerosols in the atmosphere. The ratio of absorption to scattering varies based on aerosol type. Accurate representation of that ratio is important for calculating diffuse radiation. On the other hand DNI loss estimation only requires knowledge of extinction and not the apportionment between scattering and absorption. The atmospheric constituents that impact solar radiation are the atmospheric gases and aerosols. Most atmospheric gases are well mixed and extinction of DNI resulting from those gases is easily calculated with minimal uncertainty. On the other hand the two most important variables that influence DNI but are not well mixed are aerosols and water vapor. For our study it is advantageous that aerosol and water vapor loading primarily lies in the lower troposphere with much lower concentrations generally existing above the boundary layer. As aerosol loading is high close to the surface the attenuation loss between heliostat and receivers is significantly influenced by the magnitude and variability of aerosol amount. Based on this understanding of aerosol distribution we build a model that relates attenuation losses close to the surface to

DNI measurements. This section is divided into three subsections. Section 2.1 outlines the theory used to develop a relationship between measured DNI and corresponding attenuation between heliostat and receiver in a central receiver system. Section 2.2 provides an outline of the radiative transfer model used in the calculations while Section 2.3 contains details about model inputs and the actual scenario used in this paper.

2.1 Theory

As previously mentioned we are concerned with DNI losses and do not require single scattering albedo (ratio of scattering to extinction) estimates. Therefore DNI at any height in the atmosphere can be represented as a function of the Top-of-Atmosphere DNI using the relationship.

$$DNI = DNI_{TOA} e^{-\frac{\tau}{Cos(\theta)}} \tag{1}$$

where, DNI_{TOA} is the Top-of-Atmosphere DNI, τ is the extinction optical depth of the atmospheric column and θ is the solar zenith angle. We can then use Equation 1 to defining aerosol forcing F as

$$F = \frac{DNI_a}{DNI_b} = e^{\frac{-(\tau_a - \tau_b)}{Cos(\theta)}} \tag{2}$$

where DNI_a represent the measured DNI in an atmosphere that contains aerosols while DNI_b represents a baseline theoretically calculated clean atmosphere with no aerosols for the same sun position and therefore the same zenith angle and earth to sun distance. Using Equation 2 the difference in optical depth between DNI_a (an atmosphere with aerosols) and DNI_b (a "clean" baseline atmosphere with no aerosols) can be represented as

$$X = (\tau_a - \tau_b) = -\log(F) \times Cos(\theta) \tag{3}$$

Using a relationship similar to Equation 1 we can represent the DNI at the surface as a function of the DNI received at a layer Δz above the surface. This relationship is

$$DNI_{sfc} = DNI_i e^{\frac{-\tau_{\Delta z}}{Cos(\theta)}} \tag{4}$$

where, DNI_{sfc} and DNI_i represent the DNI at the surface and a level Δz above the surface and $\tau_{\Delta z}$ represents the optical depth of the surface layer. Equation 4 can then be used to represent the optical depth of an atmospheric layer Δz that lies between the surface and any height z. The relationship is

$$Y = \tau_{\Delta z} = -\log\left(\frac{DNI_{sfc}}{DNI_i}\right) \times Cos(\theta) \tag{5}$$

2.2 Radiative Transfer Model

The radiative transfer model that we used in this study is based on the δ2 stream numerical algorithm presented by [6] and [7], which bears the acronym RAPRAD (Rapid Radiative Transfer) to signify its speed of computation. The model has 32 spectral intervals ranging from 0.24 µm to 4.6 µm in the shortwave and near-infrared, using absorption coefficients based on k distributions and a correlated-k approximation as explained in detail by [8].

The top of atmosphere spectral solar irradiance in the RAPRAD model is based on the solar irradiance of MODTRAN3[9] using the Kurucz database[10]. The RAPRAD model incorporates ozone, oxygen, carbon dioxide and water vapor absorption, as well as water vapor continuum absorption. The molecular scattering optical depth is computed using the Rayleigh optical depth calculation as shown in [11].

For RAPRAD model inputs based on high-quality measurements at the United States Department of Energy's Atmospheric Radiation Measurement (ARM) Southern Great Plains (SGP) Cloud and Radiation Testbed (CART) site measurements, calculated surface fluxes are generally within 15-20 Wm^{-2} of surface flux measurements [12].

2.3 Simulation Design

The atmospheric layers in the RAPRAD model are arbitrary and can be set according to the requirements of the problem at hand. We set the top of atmosphere at 70 km and divided the atmosphere below 16 km into 250 m thick layers. Above 16 km model layer thicknesses are set to increase with altitude. In the model simulations we use a surface albedo of 0.2 that is invariant with wavelength; this value is typical of the surface albedo of farmland in the mid-visible (e.g. Blythe, CA Typical Meteorological Year surface albedo from http://rredc.nrel.gov/solar/old_data/nsrdb/1991-2005/tmy3/). Clear-sky RAPRAD irradiance calculations require vertical profiles of pressure, temperature, water vapor, ozone, and aerosol particles. We used a mid-latitude summer atmospheric profile from MODTRAN [9] for pressure, temperature, water vapor mixing ratio and ozone profiles. Our baseline clean case contains no aerosols. For externally mixed aerosol we use mineral dust with the Angstrom exponent value [13] from [12]. The aerosol is taken to be evenly distributed in the lowest 1000 m of the atmospheric column. DNI is calculated for 0.5 degree increments with the zenith angle varying from 0-80 degrees.

3. RESULTS

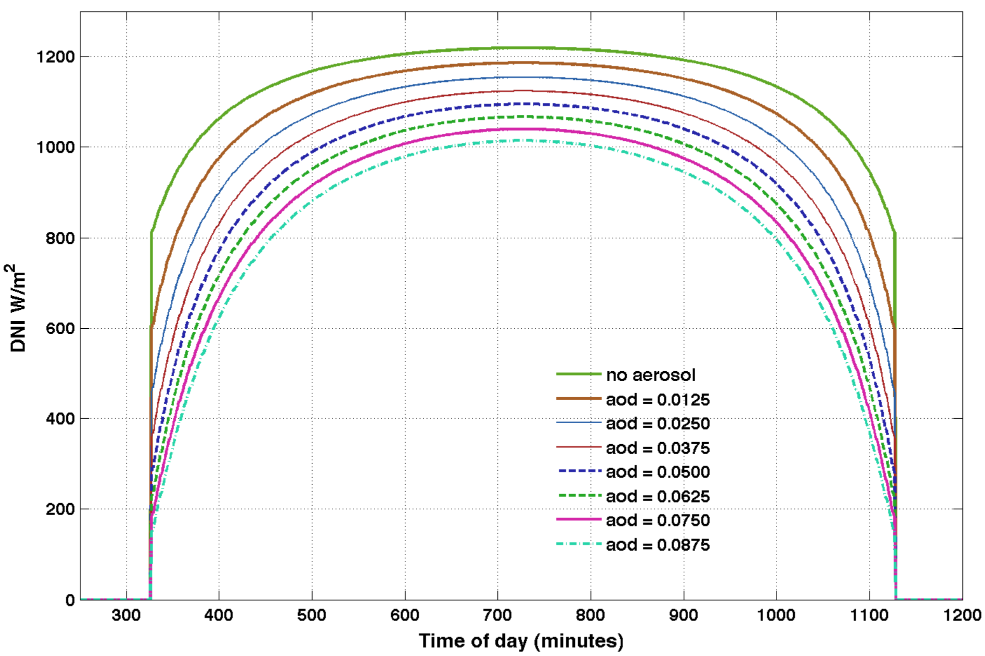

Figure 1: DNI at the surface is shown for various times of the day. The green solid line having the highest DNI for a particular time represents the case of no aerosols. An aerosol optical depth of less than 0.1 can lead to a reduction of DNI by over 200 W/m^2.

RAPRAD was run at 1-minute increments during the period of a day. For determining solar position during the time of the day we considered July 21 at Golden, CO. Calculations were done as previously mentioned for a mid-latitude summer atmospheric profile for a station assumed to be at sea level. The calculations were run for a baseline case with no aerosols as well as for various increasing levels of aerosol optical depths (AOD) ranging from 0.0125 to 0.1. RAPRAD produces DNI and Global Horizontal Irradiance (GHI) at the boundaries of every atmospheric model layer for each of the 32 spectral intervals. The broadband DNI is calculated by summing the spectral DNI. Figure 1 shows how the DNI varies during the day with each line representing various aerosol optical depths. It is seen that DNI can be reduced by around 200 W/m^2 for a change in AOD of 0.1. As all other atmospheric properties were held constant it is obvious that the reduction in DNI is a result of increase in AOD.

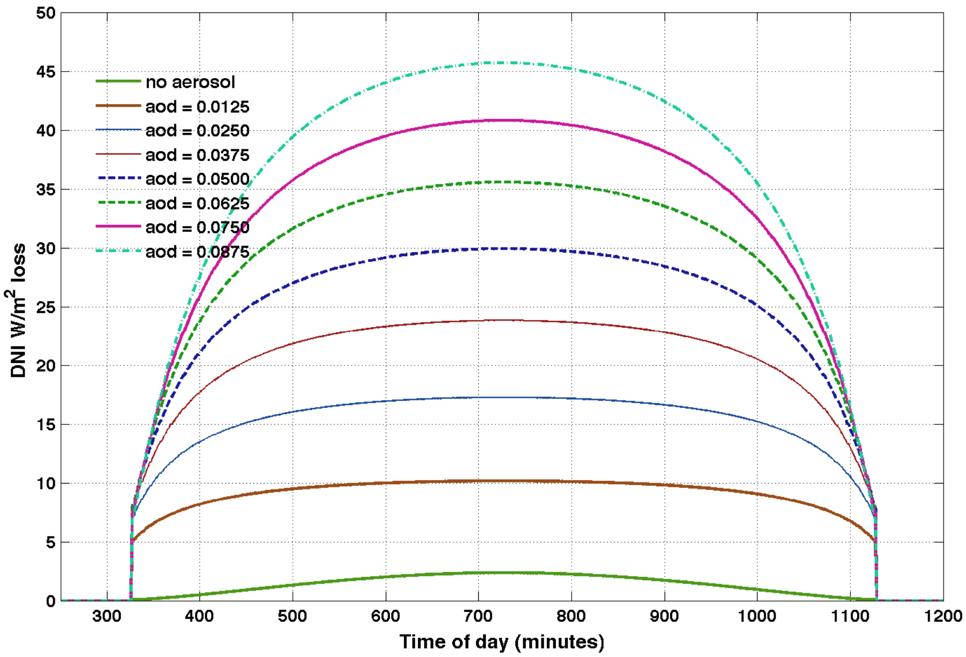

Figure 2: Attenuation of DNI in the lowest 250 m of the atmosphere for various aerosol optical depths. Note the low level of attenuation in the absence of aerosols as shown by the green solid line.

While Figure 1 shows how the DNI changes for various AOD's Figure 2 shows the attenuation in DNI in the lowest 250 m of the atmosphere where a power tower will operate. Effectively Figure 2 shows the difference in DNI at a level 250 m above the surface (not shown) and the surface (Figure 1). We can see that AOD difference of less that 0.1 can result in losses of around 40 W/m^2.

As mentioned above the goal of this work is to relate the attenuation of DNI reflected towards the receiver in the layer closest to the surface to measured DNI in the presence of aerosols. To establish this relationship we relate X (the difference between the optical depth used to calculate a baseline DNI and the optical depth of the atmosphere for a measured DNI) and Y (optical depth of the layer closest to the surface) in Equation 3 and Equation 5 respectively.

Figure 3 shows the relationship between X (the total optical depth difference calculated in Equation 3) and the Y (optical depth of the lowest 250 m atmospheric layer). The colored lines show that the relationship is fairly constant for the whole range of zenith angles if the AOD is constant. The black line is a least square fit to the means calculated for each of the various colored datasets each representing fixed AOD but varying solar zenith angles. It is obvious from Figure 3 that the relationship with the means is robust. This is borne out of the fact that the coefficient of determination (Table 1) which is an indicator of the variance that is explained by the model is nearly 100%. Figure 3 shows that there is a zenith angle dependence on the relationship be X and Y. This primarily arises from some wavelength bands becoming saturated as the airmass increases with zenith angle.

Using the relationship represented by the black line in Figure 3 we can determine the attenuation between heliostat and receiver if the distance between the two is known. The relationship in the case is represented by

$$Y = 0.2299 \times X + 0.002674 \qquad (6)$$

where Y is the optical depth of the bottom 250 m atmospheric layer. The intercept represents the in Equation 5 represents attenuation in the 250 m atmospheric layer in the absence of aerosols. Therefore if the distance *d* between heliostat and receiver is known the DNI at the receiver is

$$DNI_{rec} = DNI_{sfc} e^{\frac{Y*d}{250}} \qquad (7)$$

Statistic	Value
P1 (slope of regression fit)	0.2299 (95% confidence bounds [0.2269, 0.2329])
P2 (intercept of regression fit)	0.002674 (95% confidence bounds [0.002223, 0.003126])
Sum of squares of residuals	6.0907e-7
Coefficient of Determination R^2	0.9998

Table 1: The linear least squares fit shows that a robust relationship exists between the column optical depth difference when comparing the measured value to a clean atmosphere DNI and the optical depth of the lowest atmospheric layer (in this case 250 m).

The relationship in equation 7 is dependent on the accuracy of DNI measurement at the heliostat. Typically, for well maintained sites, DNI accuracy is +/- 2.0% , or +/-20 W out of 1000 W full scale (for very well maintained measurements). It should be noted that DNI_{sfc} in Equation 4 is the actual DNI reaching the surface while the DNI_{sfc} in Equation 7 is the DNI that is reflected from the heliostats and factors in cosine losses, shading losses, blocking losses and reflectivity.

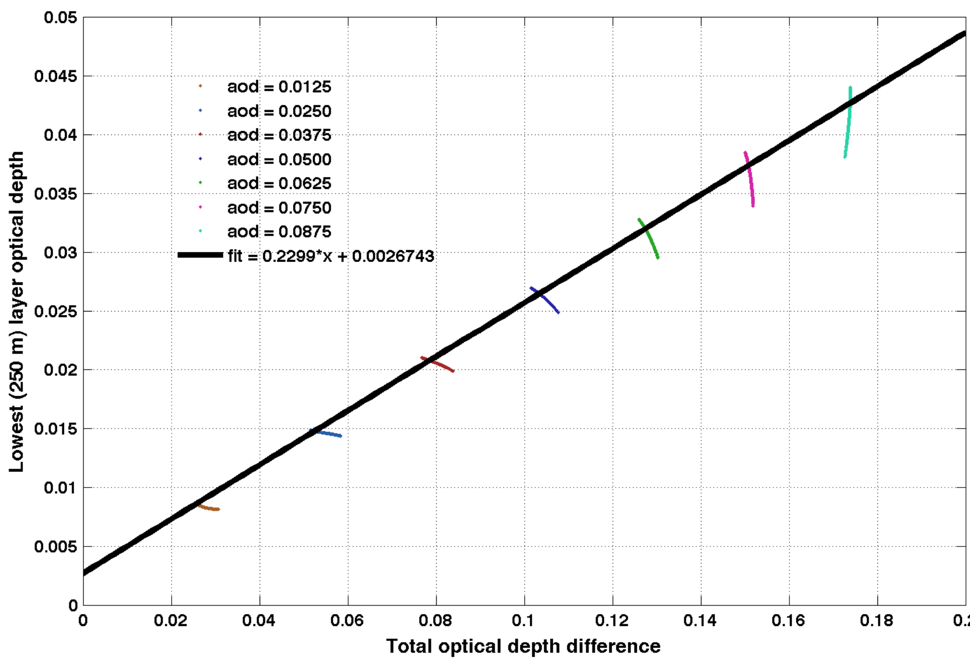

Figure 3: This figure shows how the optical depth of the lowest 250 m of the atmosphere is related to the difference in total optical depth between a clean atmosphere and an atmosphere with an aerosol optical depth represented in the legend. The black line represents the least square fit to the mean optical depth for each fixed AOD case

4. CONCLUSIONS AND FUTURE WORK

Equation 7 provides a model for attenuation losses between heliostat and receiver in a central receiver system that depends only on DNI measurements. As DNI measurements are generally available at any prospective CSP site or existing CSP plant such a model can be readily used in CSP production modeling. The model can be incorporated in available models such as the National Renewable Energy Laboratory's Solar Advisor Model (SAM).

This model relies on the fact that atmospheric constituents that are not well mixed but significantly influence DNI are primarily present close to the surface. This is especially the case of aerosols as they are primarily present below the atmospheric boundary layer. We have not investigated how sensitive the relationship we have derived is to other atmospheric profiles such as those present in the tropics. It is expected that the intercept in Equation 6 will vary to accommodate various levels of precipitable water vapor at the surface. We also have considered the case where the aerosols are uniformly distributed in the lowest 1000 m of the atmosphere. In future work our goal is to carry out the same modeling on a variety of atmospheric profiles and aerosol distributions. Additionally surface elevation needs to be accounted for to make the model applicable at all locations. As a change in surface pressure due to elevation has a linear impact on the optical depth for well-mixed gases this scaling factor will be added to the baseline DNI to make the model applicable at all elevations. Finally as previously mentioned there is a small zenith angle dependence between DNI and attenuation close to the surface. This will also be considered in our future work.

5. REFERENCES

[1] Vittitoe, C. N. and Biggs, F., 1978: Terrestrial Propagation LOSS, presented Amer. Sec. ISES meeting, Denver, August 1978, Sandia release SAND78-1137C, May 26, 1978.

[2] Hottel, H. C., 1976: A simple model for estimating the transmittance of direct solar radiation through clear atmospheres. *Solar Energy*, 18, 129-134.

[3] Leary, P.L., Hankins, J.D., 1979: A User's Guide for MIRVAL—a computer code for comparing designs of heliostat receiver optics for central receiver solar power plants. Sandia Laboratories Report, SAND77-8280, p. 14.

[4] Pitman, C.L., Vant-Hull, L.L., 1986: Performance of optimized solar central receiver systems as a function of receiver thermal loss per unit area. *Solar Energy* 37, 457–468.

[5] Schmitz, M., Shwarzbozl, P, Buck, R. and Pitz-Paal, R., 2006: Assessment of the potential improvement due to multiple apertures in central receiver systems with secondary concentrators. Solar Energy 80, 111-120.

[6] Toon, O. B., C. P. Mckay, and T. P. Ackerman, 1989: Rapid Calculation of Radiative Heating Rates and Photodissociation Rates in Inhomogeneous Multiple Scattering Atmospheres. *J. Geophys. Res.* 94, 16287–16301

[7] Kato, S., T. P. Ackerman, E. G. Dutton, N. Laulainen, and N. Larson, 1999: A comparison of modeled and measured shorwave irradiance for a molecular atmosphere. *J. Quant. Spectrosc. Radiat. Transfer* 61, 493–502.

[8] Kato, S., T. P. Ackerman, J. H. Mather, and E. E. Clothiaux, 1999: The *k*-distribution method and correlated-*k* approximation for a shortwave radiative transfer model. *J. Quant. Spectrosc. Radiat. Transfer* 62, 109–121.

[9] Berk, A., L. S. Bernstein, and D. C. Robertson: 1989: *MODTRAN: A moderate resolution model for LOWTRAN 7*, Technical Report 0122, AFGL, Geophysics Directorate/GPOS, 29 Randolph Rd., Hanscom AFB, MA 01731-3010, ADA214337.

[10] Kurucz, R. L., 1995: The solar irradiance by computation; in Proceedings of the 17th Annual Conference on Atmospheric Transmission Models, PL-TR-95-2060, G. P. Anderson, R. H. Picard, J. H. Chetwind, eds. (Phillips Laboratory Directorate of Geo-physics, Hanscom Air Force Base, Mass., 1995), pp. 333–334.

[11] Hansen, J. E. and L. D. Travis, Light Scattering in Planetary Atmospheres.: 1974: *Space Sci. Rev.* 16, 527–610.

[12] Kato, S., T. P. Ackerman, E. E. Clothiaux, J. H. Mather, G. G. Mace, M. L. Wesely, F. Murcray, and J. Michalsky, 1997: Uncertainties in modeled and measured clear-sky surface shortwave irradiances. *J. Geophys. Res.* 102, 25881–25898.

[13] Angstrom, A., 1929: On the transmission of sun radiation and on dust in air. *Geogr. Ann.* 2, 156–166.